



Contents lists available at ScienceDirect

BBA - Molecular Basis of Disease

journal homepage: www.elsevier.com/locate/bbadis

Amyotrophic lateral sclerosis associated disturbance of iron metabolism is blunted by swim training-role of AKT signaling pathway

Małgorzata Halon-Golabek^{a,1}, Damian Jozef Flis^{b,1}, Hans Zischka^{c,d}, Banu Akdogan^c, Mariusz Roman Wieckowski^e, Jędrzej Antosiewicz^{f,*}, Wiesław Ziolkowski^{g,**}

^a Department of Physiotherapy, Faculty of Health Sciences, Medical University of Gdansk, Gdansk, Poland

^b Department of Pharmaceutical Pathophysiology, Faculty of Pharmacy, Medical University of Gdansk, Gdansk, Poland

^c Institute of Molecular Toxicology and Pharmacology, Helmholtz Center Munich, German Research Center for Environmental Health, Neuherberg, Germany

^d Institute of Toxicology and Environmental Hygiene, Technical University Munich, School of Medicine, Munich, Germany

^e Laboratory of Mitochondrial Biology and Metabolism, Nencki Institute of Experimental Biology, Warsaw, Poland

^f Department of Bioenergetics and Physiology of Exercise, Faculty of Health Sciences, Medical University of Gdansk, Gdansk, Poland

^g Department of Rehabilitation Medicine, Faculty of Health Sciences Medical University of Gdansk, Gdansk, Poland

ARTICLE INFO

Keywords:

ALS
Swim training
Ferritin
AKT
Muscle iron metabolism

ABSTRACT

Swim training has increased the life span of the transgenic animal model of amyotrophic lateral sclerosis (ALS). Conversely, the progress of the disease is associated with the impairment of iron metabolism and insulin signaling.

We used transgenic hmSOD1 G93A (ALS model) and non-transgenic mice in the present study. The study was performed on the muscles taken from trained (ONSET and TERMINAL) and untrained animals at three stages of the disease: BEFORE, ONSET, and TERMINAL. In order to study the molecular mechanism of changes in iron metabolism, we used SH-SY5Y and C2C12 cell lines expression vector pcDNA3.1 and transiently transfected with specific siRNAs.

The progress of ALS resulted in decreased P-Akt/Akt ratio, which is associated with increased proteins responsible for iron storage ferritin L, ferritin H, PCBP1, and skeletal muscle iron at ONSET. Conversely, proteins responsible for iron export- TAU significantly decrease. The training partially reverses changes in proteins responsible for iron metabolism. AKT silencing in the SH-SY5Y cell line decreased PCBP2 and ferroportin and increased ferritin L, H, PCBP1, TAU, transferrin receptor 1, and APP. Moreover, silencing APP led to an increase in ferritin L and H.

Our data suggest that swim training in the mice ALS model is associated with significant changes in iron metabolism related to AKT activity. Down-regulation of AKT mainly upregulates proteins involved in iron import and storage but decreases proteins involved in iron export.

1. Introduction

Amyotrophic lateral sclerosis (ALS) is an incurable, chronic neurodegenerative disease characterized by the selective death of motoneurons in the motor cortex, brainstem, and spinal cord [1]. Disease progression is phenotypically characterized by the loss of muscle tone, paresis, muscle atrophy, and spasticity [2]. Due to the lack of a cure, all therapies tested in the field of ALS are related to prolongation and

improvement of quality of life. To achieve these goals, researchers are looking for new mechanisms related to disease progression and trying to reverse these changes. Our and other studies indicated that the development of ALS results in disrupted energy metabolism, oxidative stress, decreased muscle strength and mass, and shortness of ALS animals' lives [3–6]. Also, during ALS, impairment of iron metabolism is observed [7]. It is challenging to recognize if changes in iron metabolism are the result or a cause of the disease. The protective effects of iron chelation that extend animals' life span indicate that iron can participate in ALS

* Correspondence to: J. Antosiewicz; Department of Bioenergetics and Physiology of Exercise, Faculty of Health Sciences, Medical University of Gdansk, Dębinki 1 street, 80-211 Gdansk, Poland.

** Correspondence to: W. Ziolkowski; Department of Rehabilitation Medicine, Medical University of Gdansk, Al. Zwyciestwa 30 street, 80-219 Gdansk, Poland.

E-mail addresses: jedrzej.antosiewicz@gumed.edu.pl (J. Antosiewicz), wieslaw.ziolkowski@gumed.edu.pl (W. Ziolkowski).

¹ These authors equally contributed to this paper.

<https://doi.org/10.1016/j.bbadis.2023.167014>

Received 25 August 2023; Received in revised form 8 December 2023; Accepted 27 December 2023

Available online 1 January 2024

0925-4439/© 2023 Published by Elsevier B.V. This article is made available under the Elsevier license (<http://www.elsevier.com/open-access/userlicense/1.0/>).

Abbreviations

AKT	protein kinase B
ALS	Amyotrophic lateral sclerosis
APP	amyloid-beta precursor protein
FPN1	ferroportin
LIP	labile iron pool
NTg	non-transgenic
p-AKT	active form of protein kinase B
PCA	principal components analysis
PCBP1	Poly(RC) Binding Protein 1
PCBP2	Poly(RC) Binding Protein 2
SEM	standard error of the mean
TfR1	transferrin receptor 1

pathology [8]. One of the main characteristics of the changes in iron metabolism is its accumulation in skeletal muscle and neuronal tissue [6,7]. Excess iron accumulation and its redox activity can lead to the formation of free radicals and cause cell damage. Nevertheless, the mechanism of tissue iron accumulation is not well understood. Proteins involved in cellular iron metabolism can be divided into those involved in iron import (transferrin receptor 1 (TfR1), Poly(RC) Binding Protein 1 (PCBP1), intercellular storage and trafficking (ferritin L and ferritin H, divalent metal transporter 1), and iron export (ferroportin, (FPN1), Poly (RC) Binding Protein 2 (PCBP2), amyloid-beta precursor protein (APP), TAU, hephaestin, ceruloplasmin). Interestingly, some of these proteins regulate iron metabolism and play an essential role in many other processes like RNA processing, gene expression, microtubule transport, etc. [9,10]. Besides, excess tissue iron accumulation is associated with iron-dependent oxidative stress, which can deleteriously influence signaling pathways [11]. Thus, knowing the mechanism of tissue iron accumulation seems crucial for understanding ALS's pathomechanism and possibly other diseases.

Mutation in the genes encoding some of the proteins involved in iron metabolism has been shown to cause neurodegeneration in the central nervous system [12]; however, iron accumulation could also be a result of impairing intracellular signaling pathways. Recently, we postulated that the weakening protein kinase B (AKT) signaling pathway regulates iron metabolism [13]. A decreased AKT activity in ALS skeletal muscle was associated with iron accumulation [6]. Besides, the downregulation of AKT in several cell cultures leads to increased intracellular ferritin, a sensitive indicator of cellular iron status [14]. Conversely, iron accumulation can lead to AKT inactivation [15,16]. AKT includes a family of three closely related cellular homologs: AKT1, AKT2, and AKT3. The encoded proteins are serine/threonine kinases, which regulate cell growth, cell proliferation and survival, glucose metabolism, angiogenesis, and others [17].

Conversely, there is no data on whether these effects due to the loss of AKT activity will be related to changes in proteins responsible for iron import and export.

Recently, we showed that the AKT signaling pathway, which is partly responsible for skeletal muscle atrophy, was modulated during ALS. Swim training may partially reverse these changes [3]. Besides these facts, swim training is one of the best therapy for ALS. An increasing number of studies suggest that swim training prolongs the lifespan of ALS mice, with an accompanying improvement in muscle bioenergetics and glucose metabolism and a reduction of muscle fiber loss and weight [3,4,18]. In addition, recently, we have shown that swim training attenuates the reduction of muscle strength in ALS mice and positively influences the function of skeletal muscle mitochondria [5,6]. However, according to our knowledge, there is no information on whether this therapy also affects iron metabolism. Several studies demonstrate that physical activity reduces body iron accumulation, but the exact mechanisms are unknown [19,20]. Thus, we assumed that if iron plays an essential role in the pathogenesis of ALS, then swim training should protect against its excessive accumulation in skeletal muscles and reverse changes in proteins of iron metabolism. Therefore, this study aimed to examine the protective mechanism of swim training in a transgenic animal model of ALS and the role of AKT signaling pathways in iron metabolism.

We hypothesized that ALS modulates proteins involved in skeletal muscles' iron metabolism and that these changes are related to the inactivation of AKT protein.

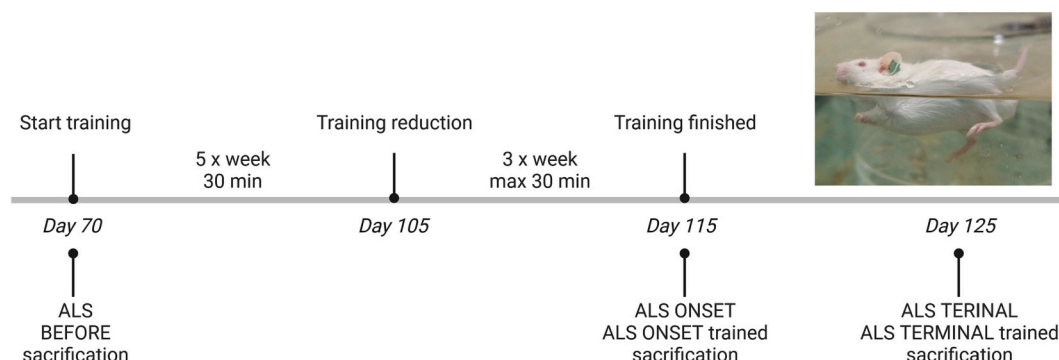
Here, we report that swim training significantly modulates proteins involved in skeletal muscle's iron metabolism, and the changes can explain lower iron accumulation. Changes in proteins of iron metabolism in transgenic animals are partially mirrored in cells where AKT has been silenced.

2. Materials and methods

2.1. Animals

All experimental procedures were performed in accordance with European animal research laws (European Communities Council Directive 1986/609/EEC). The experiments with animals were approved by the Local Ethics Committee (Resolution No. 11/2013) and the Polish Ministry of the Environment (Decision No. 155/2012). The study was carried out in compliance with the ARRIVE guidelines.

Transgenic male B6SJL-Tg 1Gur/J mice with the human SOD1 G93A mutation (SOD1G93A) (ALS mice) (five groups, $n = 5$ per group) and wild-type, non-transgenic, male B6SJL mice serving as a controls (NTg, $n = 5$) were purchased from the Jackson Laboratory (Bar Harbor, ME, USA). The mice were housed behind a sanitary barrier in a controlled environment at 23 ± 1 °C and 50–60 % relative humidity, under a 12-h light-dark cycle and specific pathogen-free status. Food and water were available ad libitum. After 14 days of acclimatization, the mice were



Scheme 1. The experimental design

randomly divided into the following groups according to the disease progression and training status: ALS BEFORE: ALS untrained mice with no visible signs of the disease; ALS ONSET: ALS untrained and trained groups of mice; ALS TERMINAL: ALS untrained and trained groups of mice, as described previously [21].

The mice were euthanized by cervical dislocation. The mice from the ALS BEFORE group were euthanized on the 70th day of life. The mice from both ALS ONSET groups were euthanized when we observed the first disease symptoms in the untrained group (115 ± 2 days of life). Both ALS TERMINAL groups of mice were euthanized after observing, in untrained groups of mice, functional paralysis in both hind legs, and animals could not right within 30 s after we placed them on their side. (125 ± 2 days of life) [22], as shown in Scheme 1. The calf muscles were removed from both hind limbs, dissected from fat and connective tissue, and frozen in liquid nitrogen.

2.2. Swim training protocol

ALS mice (ALS ONSET trained and ALS TERMINAL trained) started the training procedure at 10 weeks of age, as per [4], with the slight modification described by [6]. A unique pool with regulated water flow was used to conduct the swim training. To reduce the stress of animals related to the liquid environment, each animal from the trained groups underwent 5 day acclimatize protocol: day 1–5 min in the water, day 2–15 min in the water, day 3–25 min in the water, day 4–30 min with low water flow and from day 5–30 min with normal water flow.

Mice were swimming 5 times a week for 30 min. The water temperature was 30 °C, with a maximum flow speed of 5 L/min (every time the water flow increased from the beginning of training, and the lowest water flow forcing animals to swim was chosen for the session). The training frequency was reduced to 3 times a week at 105 days of age. According to the individual mice's capabilities, exercise times were specially adapted (from 105 days of age, mice had problems with long-time swimming; therefore, the session was ended sooner if mice could not swim). The training finished at 115 days of life, as shown in scheme 1.

2.3. Tissue homogenization

Following the dissection performed at 4 °C, the tissue samples were kept at –80 °C. For experiments, weighed pieces of tissue were homogenized using a glass Teflon homogenizer (10 % wt/vol) in RIPA lysis buffer (Sigma Aldrich, Cat. No. R0278) supplemented with protease inhibitor (Roche, Cat No. 4693159001) and phosphatase inhibitor (Roche, Cat. No. 04906837001). After homogenization, the lysates were frozen at –70 °C and thawed at 30 °C thrice. Lastly, using the Sigma 3 K30 centrifuge, the samples were centrifuged at $15,000 \times g$ at 4 °C for 10 min. The supernatants were transferred to fresh tubes and frozen at –80 °C for further analysis.

2.4. Cell culture

The cells were cultured in a growth medium consisting of high glucose DMEM (for SHSY-5Y: DMEM/F12- PAN-Biotech, Cat. No. P04-41250; for C2C12: Sigma Aldrich, Cat. No. D6429), 10 % (vol/vol) fetal bovine serum (Sigma Aldrich Cat. No. F9665), 100 U/mL penicillin, and 100 µg/mL streptomycin (Sigma Aldrich Cat. No. P4333). The cells were maintained at 37 °C in an atmosphere of 95 % air and 5 % CO₂.

Expression vector pcDNA3.1 was kindly provided by Blirt S.A (Bio-Lab Innovative Research Technologies, Gdansk, Poland). For the treatment procedure, cells were seeded at a 1.5×10^6 per 6 cm plate and allowed to attach overnight. According to the manufacturer's procedure, the cells were transiently transfected the next day.

2.5. Small interfering RNA transfection

siRNA transfection was performed according to the manufacturer siRNA transfection protocol (Santa Cruz Biotechnology). The cells were seeded at a 1.5×10^6 per 6 cm plate density and allowed to attach overnight. At 50 % to 60 % confluence, the mix of each siRNA duplex (siRNA control (Santa Cruz Biotechnology Cat. No. sc37007), AKT1 (Santa Cruz Biotechnology Cat. No. sc29196), AKT2 (Santa Cruz Biotechnology Cat. No. sc38910), AKT3 (Santa Cruz Biotechnology Cat. No. sc38912) and APP (Santa Cruz Biotechnology Cat. No. sc29678)) and siRNA Transfection Reagent was administered. Five hours after transfection, the cells were supplied with the medium containing antibiotics and 20 % FBS. On the following day (20 h after medium addition), the media were replaced with fresh ones. Forty-eight hours after transfection, cells were harvested for assays. The assessment of the effect of AKT kinase silencing (siRNA AKT1, AKT2, AKT3) and APP silencing (siRNA APP) on the proteins of iron metabolism was accompanied by controlling the efficiency of the knockdown.

2.6. Cell lysate

SH-SY5Y and C₂C₁₂ stable cell lines were treated as described previously [13]. Both floating and attached cells were collected, washed in phosphate-buffered saline, and resuspended in a lysis solution containing 50 mmol/L Tris-HCl (pH 7.5), 150 mmol/L NaCl, 1 % Triton X-100, 0.1 % sodium dodecyl sulfate, and incubated for 40 min on ice with gentle shaking. The cell lysate was cleared by centrifugation at 16000 g for 20 min and kept on ice to carry out the following procedure.

2.7. Immunoblotting

In order to assess protein composition in cell lysates, equal amounts of total protein were separated into 12 %, 10 %, or 7.5 % polyacrylamide gels (according to the molecular weight of the protein) and transferred onto poly(vinylidene difluoride) membrane. Membranes were blocked in the blocking buffer 5 % (w/vol) non-fat dry milk in TBST (150 mM NaCl, 10 mM TRIS, 0.1 % Tween 20, pH = 7) for 1 h at room temperature. Next, the membranes were washed out in TBST and incubated with primary antibodies in the blocking buffer while gently shaken overnight at 4 °C.

We used the following mouse monoclonal immunoglobulin G (IgG) antibodies: AKT 1/2/3 (Santa Cruz Biotechnology Cat. #sc-81,434, 1:500), APP (Merck Millipore Cat. #MAB348, 1:1000). Additionally, the following rabbit polyclonal IgG antibodies were used: AKT 1/2/3 (Cell Signaling Cat. #4691, 1:1000), P-AKT 1/2/3 (Ser473) (Cell Signaling Cat. #4060, 1:1000), P-AKT 1/2/3 (Ser473) (Santa Cruz Biotechnology Cat. sc-7985-R, 1:500), APP (Cell Signaling Cat. #2452, 1:1000), Ferritin L (Abcam #ab69090, 1: 1000), Ferritin H (Cell Signaling Cat. #3998, 1:1000), Ferritin H (Abcam #ab65080, 1: 1000), PCBP1 (Cell Signaling Cat. #8534, 1:1000), PCBP2 (Cell Signaling Cat. #83017, 1:1000), SLC40A1 (Bioss Cat. #3579, 1:1000), Transferrin Receptor (Abcam #214039, 1:1000), Tau (Cell Signaling Cat. #46687, 1:1000).

The following antibodies were obtained from Sigma and were incubated for 1 h at room temperature with gentle shaking: anti-β-actin (Cat. #A3854, 1:50000) and secondary antibodies: anti-Rabbit IgG-Peroxidase (Cat. #A9169, 1:25000) and anti-Mouse IgG-Peroxidase (Cat. #A9044, 1:25000). After washing, the membranes were incubated with secondary anti-Rabbit IgG-Peroxidase or anti-Mouse IgG-Peroxidase conjugated antibodies. Immunoreactive bands were visualized using enhanced chemiluminescence ECL Plus (Perkin Elmer, Cat. #NEL 103001EA) and Hyper film ECL (Amersham Bioscience, Cat. #28906837). The membranes were stripped and probed using an anti-β-actin antibody as a loading control, or in the case of the phosphoforms, re-probed using antibodies raised against the non-phosphorylated forms of the proteins. Changes in protein levels were assessed by densitometry of immunoreactive bands and followed by

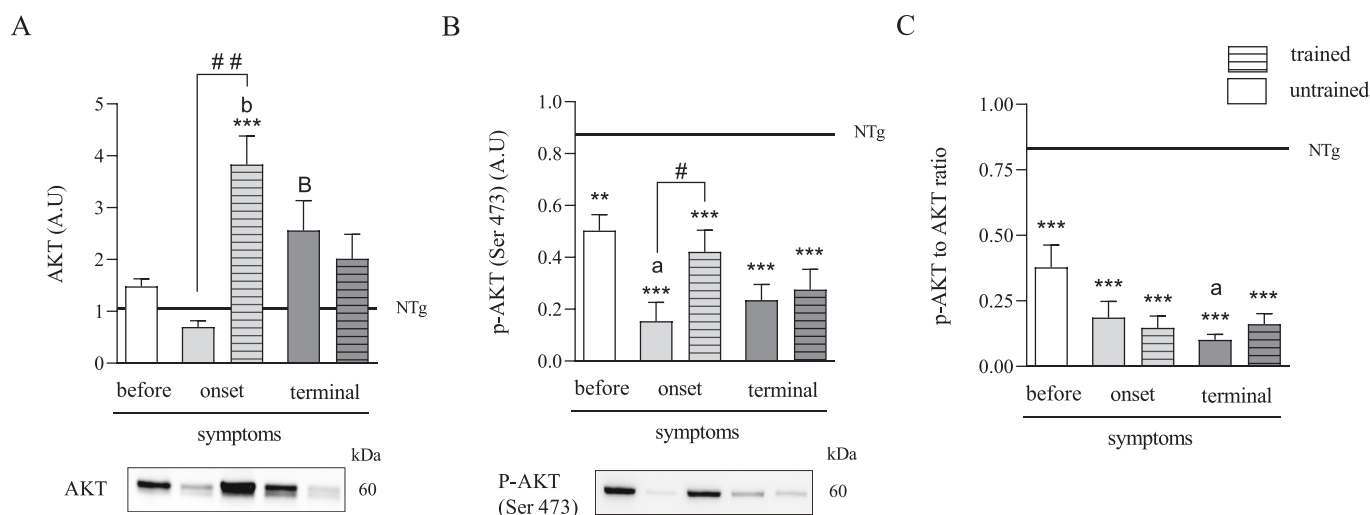


Fig. 1. Effects of swim training and ALS progression on AKT signaling pathway in skeletal muscle. AKT (A), p-AKT (Ser 473) (B), and p-AKT to AKT ratio (C) were measured in the calf-hind limb muscle. There were significant differences between groups: [#] $p < 0.05$, ^{##} $p < 0.01$ between indicated group (Mann-Whitney-test for AKT and Student *t*-test for p-AKT). ^{**} $p < 0.01$, ^{***} $p < 0.001$ vs. NTg group of mice, ^a $p < 0.05$, ^b $p < 0.01$, vs. BEFORE group ^B $p < 0.01$ vs. ONSET untrained group of mice (Tukey's post-hoc test). The data are presented as the means \pm SEM ($n = 5$ in each group).

normalization relative to the β -actin as a loading control or non-phosphorylated (for phosphorylated proteins only) protein levels.

In order to assess protein composition in skeletal muscle lysate, all procedures were conducted using the Bio-Rad Stain-Free Western Blotting Protocol. Equal amounts of total protein were separated on gradient 4–15 % Mini-PROTEAN TGX Stain-Free Protein Gels and transferred onto LF PVDF membranes. Membranes were blocked in the EveryBlot Blocking Buffer for 15 min at room temperature. Next, the membranes were washed (5x5min) out in TBST and incubated with primary antibodies in the EveryBlot blocking buffer while gently shaken overnight at 4 °C. Changes in protein levels were assessed by densitometry of the immunoreactive bands. Then, it was normalized to the total amount of protein in the samples measured on the membranes after the transfer using the Stain-free technology. All assessments were done using Image Lab 6.1 software (Bio-Rad Laboratories, Inc). Each result of the densitometry was normalized to the selected NTg animal.

2.8. Determination of iron concentrations

Iron levels in skeletal muscle homogenates were analyzed by Inductively Coupled Plasma Optical Emission Spectrometry (ICP-OES, Ciro Vision, SPECTRO Analytical Instruments GmbH) after wet-washing of samples with 65 % nitric acid (Merck) as previously described [23]. The concentration of iron in the skeletal muscle homogenates was expressed as $\mu\text{g}/\text{mg}$ protein.

2.9. Proteomic analysis

The levels of 8 investigated proteins (Transferrin receptor protein 1 TFR1; Poly(rC)-binding protein 1 PCBP1; Poly(rC)-binding protein 2 PCBP2; Microtubule-associated protein tau TAU; Amyloid beta A4 protein A4; Hephaestin-like protein 1 HPHL1; Ferritin heavy chain 1 FRIL1; Ferritin heavy chain FRIH) were determined in ALS BEFORE, ALS TERMINAL, untrained and trained groups using liquid chromatography MS3 spectrometry (LC-MS/MS) at the Thermo Fisher Center for Multiplexed Proteomics (Department of Cell Biology, Harvard Medical School, Cambridge, MA, USA). The preparation of samples (the tibialis anterior muscle) was described previously in [24]. An Orbitrap Fusion mass spectrometer (Thermo Fisher Scientific Inc., Waltham, MA, USA) and LC-MS3 data collection strategy were used to analyze the peptide fractions. A free software environment for statistical computing and graphics was chosen to visualize the changes between all studied groups.

To perform the principal component analysis (PCA), the R Statistical Software (Foundation for Statistical Computing, Vienna, Austria) was used.

2.10. Data analysis

Statistical analysis was performed using the Statistica software package (Statistica v. 12.0, StatSoft Inc. Tulsa, OK, USA).

The results are expressed as the mean \pm standard error of the mean (SEM). The normality of distribution and similarity of variances were tested to determine which statistical test should be used. The differences associated with disease progression and between ALS and NTg groups were analyzed using one-way analysis of variance (ANOVA) or the Kruskal–Wallis test. If a difference was detected in these test models, the significance level was determined using Tukey's post-hoc test. To verify the significance of swim training-associated changes (ONSET untrained vs. trained and TERMINAL untrained vs. trained), the student's *t*-test or Mann–Whitney *U* test was used. The results were considered statistically significant at $p < 0.05$.

3. Results

3.1. The effect of swim training on the Akt signaling pathway in ALS skeletal muscle

AKT levels were significantly higher in trained ALS mice at the ONSET stage of the disease (3.83 ± 0.55 A.U.) than in NTg mice (1.06 ± 0.04 A.U., $p = 0.0004$). In the TERMINAL untrained group, AKT levels were significantly higher than those in the ONSET untrained group (2.56 ± 0.57 and 0.30 ± 0.12 A.U., respectively, $p = 0.0051$). There was also an increase in AKT levels related to swim training at ONSET-stage disease ($p = 0.0051$, Fig. 1A).

The level of the active form of AKT (p-AKT Ser 473) was significantly lower in all ALS groups of mice (0.50 ± 0.06 , 0.15 ± 0.07 , 0.42 ± 0.08 , 0.23 ± 0.06 and 0.27 ± 0.08 A.U. in ALS BEFORE, ONSET untrained, ONSET trained, TERMINAL untrained and TERMINAL trained groups, respectively,) than in NTg mice (0.87 ± 0.05 A.U., $p = 0.0080$, $p = 0.0001$, $p = 0.0009$, $p = 0.0001$ and $p = 0.0001$, respectively). In the ONSET untrained group, p-AKT levels were significantly lower than those in the BEFORE group (0.15 ± 0.07 and 0.50 ± 0.06 A.U., respectively, $p = 0.0051$). There was also an increase in p-AKT level related to swim training at ONSET-stage disease ($p = 0.0368$, Fig. 1B).

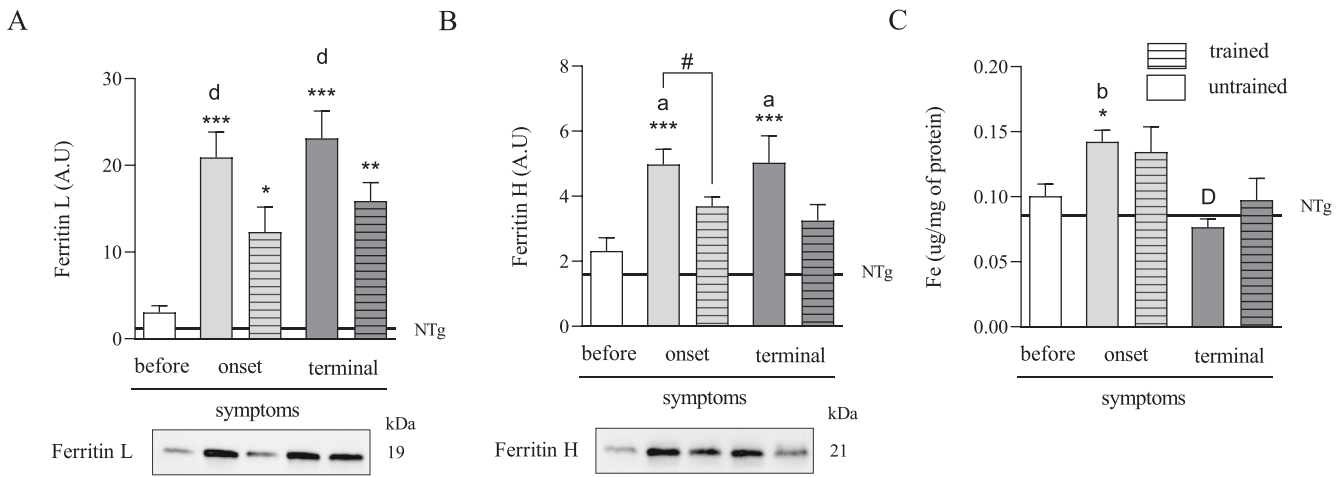


Fig. 2. Effects of swim training and ALS progression on the iron level and storage proteins in muscle. Ferritin L (A), ferritin H (B), and iron protein level (C) were measured in the calf-hind limb muscle. There were significant differences between groups: # $p < 0.05$ between indicated groups (Student t-test). * $p < 0.05$, ** $p < 0.01$, *** $p < 0.001$ vs. NTg group of mice, ^a $p < 0.05$, ^b $p < 0.01$, ^d $p < 0.001$ vs. BEFORE group ^D $p < 0.001$ vs. ONSET untrained group of mice (Tukey's post-hoc test). The data are presented as the means \pm SEM (n = 5 in each group).

The p-AKT to AKT ratio was significantly lower in all ALS groups of mice (0.38 ± 0.08 , 0.19 ± 0.06 , 0.15 ± 0.04 , 0.10 ± 0.02 and 0.16 ± 0.03 A.U. in ALS BEFORE, ONSET untrained, ONSET trained, TERMINAL untrained and TERMINAL trained groups, respectively) than in NTg mice (0.83 ± 0.04 A.U., $p = 0.0001$, $p = 0.0001$, $p = 0.0001$, $p = 0.0001$ and $p = 0.0001$, respectively). In the TERMINAL untrained group, p-AKT to AKT levels were significantly lower than those in the BEFORE group (0.10 ± 0.02 and 0.38 ± 0.08 A.U., respectively, $p = 0.0167$, Fig. 1C).

3.2. The effect of swim training on iron-dependent protein level in ALS skeletal muscle

Ferritin L levels were significantly higher in untrained and trained ALS mice at the ONSET and TERMINAL stages of the disease (20.92 ± 2.91 , 12.30 ± 2.90 , 23.12 ± 3.15 and 15.88 ± 2.12 A.U., respectively in ONSET untrained, ONSET trained, TERMINAL untrained and

TERMINAL trained groups of mice) than in NTg mice (1.23 ± 0.10 A.U., $p = 0.0001$, $p = 0.0217$, $p = 0.0001$ and $p = 0.0013$). Untrained ALS mice at the ONSET and TERMINAL stage of the disease also had higher ferritin L levels than the ALS BEFORE group (3.03 ± 0.78 A.U., $p = 0.0005$ and $p = 0.0003$). There was a tendency to decrease ferritin L protein levels at the ONSET and TERMINAL stages of ALS related to swim training ($p = 0.062$ and $p = 0.086$, for ONSET and TERMINAL groups, respectively Fig. 2A).

Ferritin H levels were significantly higher in untrained ALS mice at the ONSET and TERMINAL stage of the disease (4.98 ± 0.46 and 5.03 ± 0.83 A.U., respectively) than in NTg mice (1.06 ± 0.04 A.U., $p = 0.0006$ and $p = 0.0005$). Untrained ALS mice at the ONSET and TERMINAL stage of the disease had higher ferritin H levels than the ALS BEFORE group (2.32 ± 0.41 A.U., $p = 0.0170$ and $p = 0.0151$). Swim training lowers ferritin H levels at the ONSET stage (3.69 ± 0.29 A.U. in ONSET trained group, $p = 0.0401$), and there was a tendency to decrease this protein level at the TERMINAL stage (3.25 ± 0.50 A.U., $p = 0.0948$,

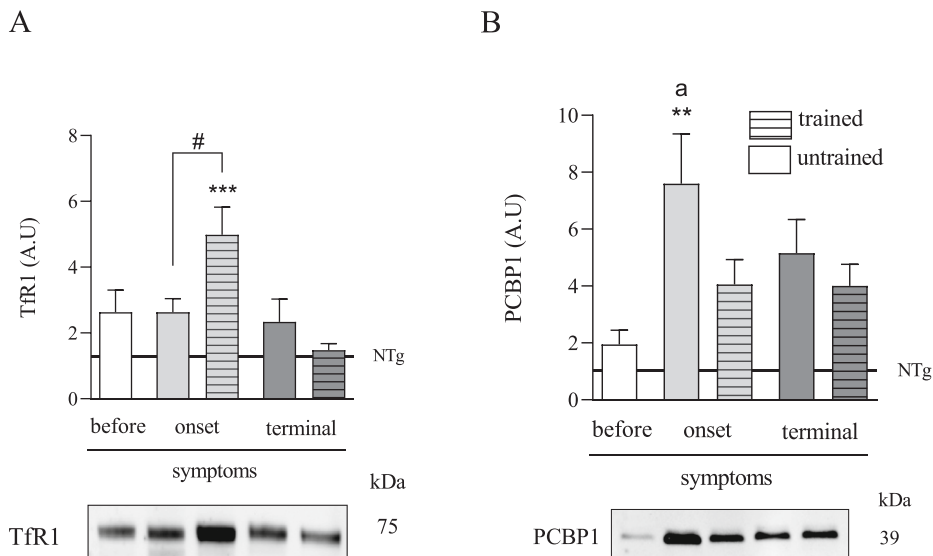


Fig. 3. Effects of swim training and ALS progression on iron import proteins in skeletal muscle. TfR1 (A) and PCBP1 (B) were measured in the calf-hind limb muscle. There were significant differences between groups: # $p < 0.05$ between indicated groups (Student t-test). ** $p < 0.01$, *** $p < 0.001$ vs. NTg group of mice, ^a $p < 0.05$ vs. BEFORE group of mice (Tukey's post-hoc test). The data are presented as the means \pm SEM (n = 5 in each group).

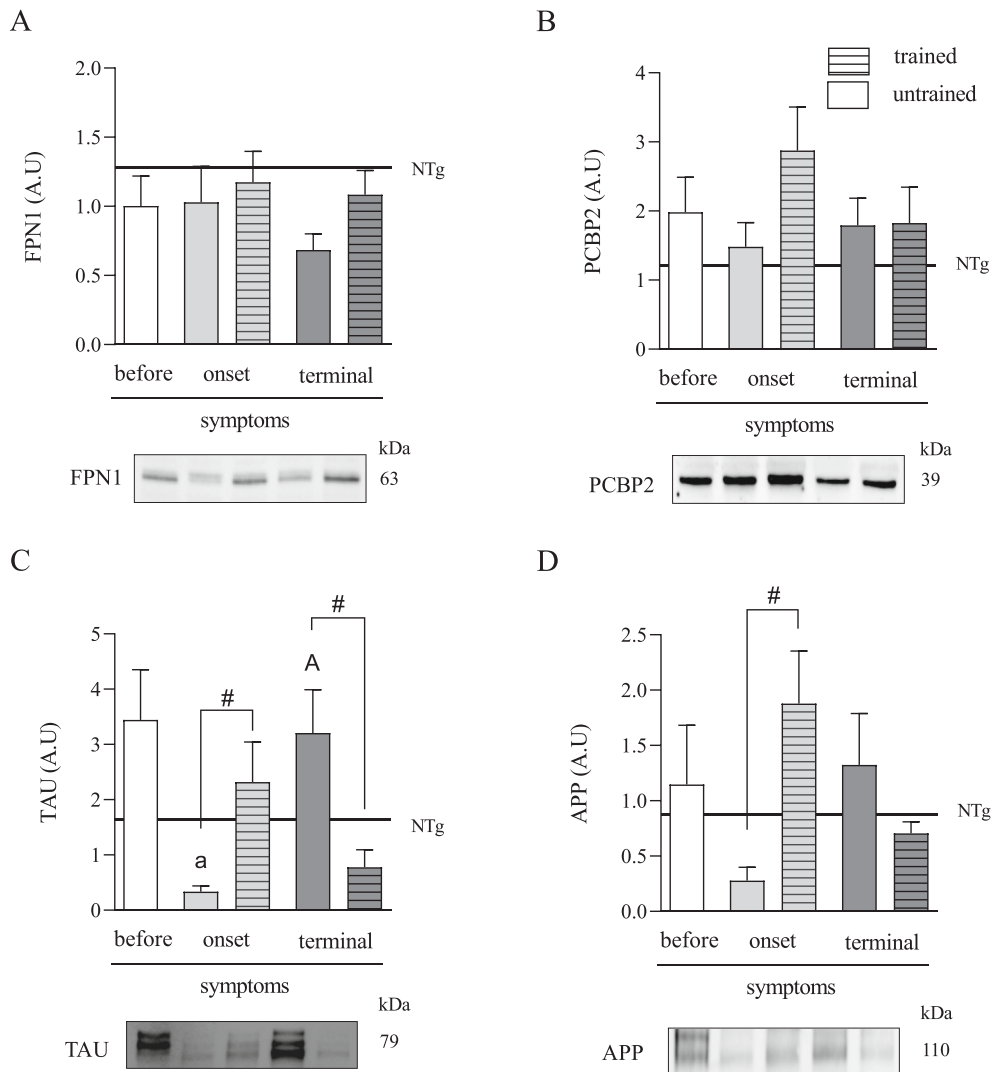


Fig. 4. Effects of swim training and ALS progression on iron export proteins in skeletal muscle.

FPN1 (A), PCBP2 (B), TAU (C), and APP (D) were measured in the calf-hind limb muscle. There were significant differences between groups: # $p < 0.05$ between indicated groups (Mann-Whitney-test). ^a $p < 0.05$ vs. BEFORE group, ^A $p < 0.05$ vs. ONSET untrained group of mice (Tukey's post-hoc test). The data are presented as the means \pm SEM ($n = 5$ in each group).

Fig. 2B).

The Fe concentration in skeletal muscle increased in the untrained ONSET group (0.142 ± 0.009 $\mu\text{g}/\text{mg}$ of protein) in comparison to the NTg group (0.086 ± 0.005 $\mu\text{g}/\text{mg}$ of protein, $p = 0.0274$). Untrained ONSET ALS mice also had a higher concentration of Fe than the ALS BEFORE group (0.100 ± 0.009 $\mu\text{g}/\text{mg}$ of protein, $p = 0.0071$). At the TERMINAL stage of ALS, the untrained group had a decreased concentration of Fe (0.076 ± 0.006 $\mu\text{g}/\text{mg}$ of protein) than the untrained ONSET group ($p = 0.0003$, Fig. 2C).

3.3. Effects of swim training and ALS progression on iron import proteins in skeletal muscle

The TfR1 level in skeletal muscle increased in the trained ONSET group (4.98 ± 0.84 A.U.) compared to the NTg group (1.27 ± 0.24 A.U., $p = 0.0009$) and to the untrained ONSET group (2.63 ± 0.41 A.U., $p = 0.0312$, Fig. 3A).

The PCBP1 level in skeletal muscle increased in the untrained ONSET group (7.60 ± 1.75 A.U.) compared to the NTg group (1.05 ± 0.10 A.U., $p = 0.0010$). Untrained ONSET ALS mice also had higher PCBP1 levels than in the BEFORE group (1.94 ± 0.50 A.U., $p = 0.0160$, Fig. 3B).

3.4. The effect of swim training on iron-exporting protein level in ALS skeletal muscle

There were no changes in any of the analyzed groups in the skeletal muscles, either in FPN1 or PCBP2 (Fig. 4A and B).

Untrained ALS mice at the ONSET stage of the disease had lower TAU levels (0.34 ± 0.10 A.U.) than the ALS BEFORE group (3.4 ± 0.90 A.U., $p = 0.0165$). Interestingly, in untrained animals at the TERMINAL stage of the disease, the TAU protein level increased (3.20 ± 0.78 A.U.) compared to the untrained ONSET ALS group ($p = 0.0267$). At different stages of the disease, there was also an opposite response to swim training. At ONSET, swim training led to the TAU level increase (2.32 ± 0.72 A.U., $p = 0.0131$), and at the TERMINAL stage, there was a decreased level of TAU in the trained ALS group (0.78 ± 0.32 A.U., $p = 0.0166$, Fig. 4C).

There were no changes in the APP level either in NTg mice or during the progression of the disease. However, there was a significant increase related to swim training at the ONSET stage of the disease (0.28 ± 0.12 and 1.88 ± 0.47 A.U., in ONSET untrained and trained ALS mice, respectively, $p = 0.0306$, Fig. 4D).

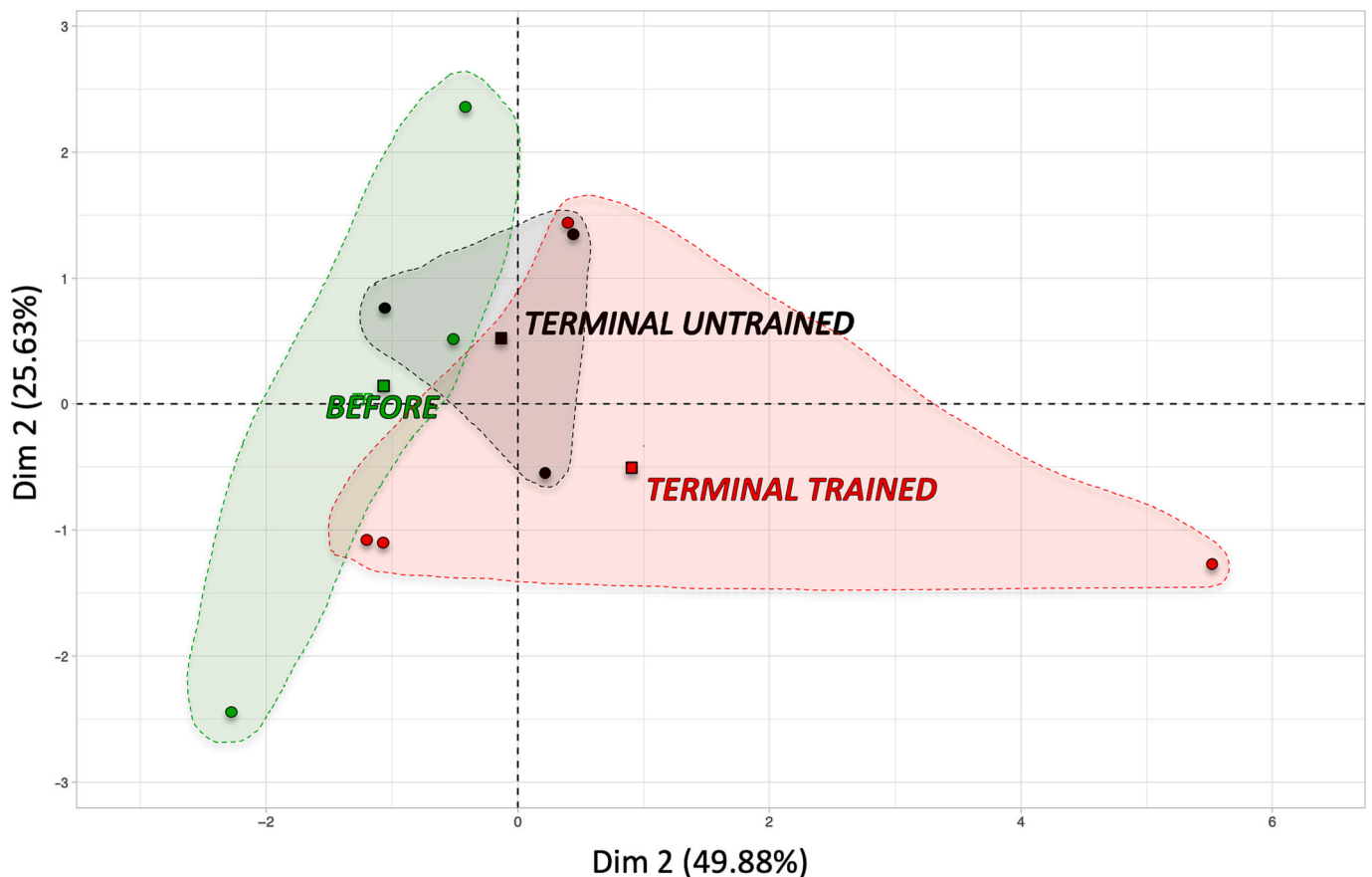


Fig. 5. Principal component analysis presenting the profile of iron metabolism proteins.

The 2D graph of variables PC1 and PC2 created using PCA based on the level of 8 identified proteins: (Transferrin receptor protein 1 TFR1; Poly(rC)-binding protein 1 PCBP1; Poly(rC)-binding protein 2 PCBP2; Microtubule-associated protein tau TAU; Amyloid beta A4 protein A4; Hephaestin-like protein 1 HPHL1; Ferritin light chain 1 FRIL1; Ferritin heavy chain FRIH) in the skeletal muscle of the BEFORE, TERMINAL untrained, and TERMINAL trained mice.

3.5. The effects of swim training on Fe metabolism proteomic profiles of ALS mice skeletal muscle

To evaluate the effect of swim training on the levels of proteins involved in Fe metabolism, we performed a comparative proteomic analysis of mice skeletal muscle at the Thermo Fisher Center for Multiplexed Proteomics. The proteomic analysis allows us to identify 8 proteins related to the Fe metabolism: (Transferrin receptor protein 1 TFR1; Poly(rC)-binding protein 1 PCBP1; Poly(rC)-binding protein 2 PCBP2; Microtubule-associated protein tau TAU; Amyloid beta A4 protein A4; Hephaestin-like protein 1 HPHL1; Ferritin light chain 1 FRIL1; Ferritin heavy chain FRIH). In order to visualize possible similarities or differences in the proteomic profiles of proteins related to the Fe metabolism in BEFORE, TERMINAL untrained, and TERMINAL trained groups, we performed principal component analysis (PCA). PCA allowed us to extract the important information from multivariate data (level of 8 individual proteins) and to express this information as a set of lower number new variables called principal components (PC). In this case, PCA transformed 8 variables (the levels of individual above-listed proteins related to the Fe metabolism) into two- or three principal components, retaining the maximum information about the level of individual proteins taken for the analysis. In other words, PCA reduced the dimensionality of multivariate proteomic data to two or three PCs, which can be easier visualized graphically (two or three-axis graph), with minimal loss of information regarding levels of individual proteins related to the Fe metabolism (see Fig. 5 and Fig. S1). Differences in the localization of the individual experimental groups in two-dimensional space indicate divergences in the “Fe metabolism proteomic profiles”

of BEFORE, TERMINAL untrained, and TERMINAL trained groups (Fig. 5). Additionally, three-dimensional space presentation of the results (3D graph) shows better that the Fe metabolism proteomic profile differs among the studied groups (Fig. S1.). This suggests that the TERMINAL untrained Fe metabolism signature (fingerprint created based on the proteomic profile of proteins related to the Fe metabolism) differs from those obtained for BEFORE and TERMINAL trained groups.

3.6. Effects of siRNA against AKT1, AKT2, and AKT3 on AKT protein level in SH-SY5Y and C₂C₁₂ cell lines

We decided to test whether the impairment of signaling downstream of insulin receptors would induce changes in iron metabolism. Thus, we transfected SH-SY5Y and C₂C₁₂ cell lines with siRNA against AKT1, AKT2, and AKT3, respectively. As shown in Fig. 6, transfection led to the down-regulation of all three isoforms of the kinases in both cell lines (Fig. 6, Fig. S2).

3.7. Effects of AKT silencing on proteins involved in iron import and storage in SH-SY5Y and C₂C₁₂ cell lines

As shown in Fig. 6, transfection led to the down-regulation of the kinase, which increased the level of both ferritin subunits (Fig. 7 A and B). The highest increase of ferritin was observed in siRNA AKT 3 in both cell lines. The level of ferritin L for siAKT 2 and 3 was 1.3 ± 0.29 and 1.45 ± 0.38 A.U. in the SH-SY5Y cell line (Fig. 7A), and 1.3 ± 0 and 1.43 ± 0.25 A.U. in C₂C₁₂ cell line (Fig. S3 A). The increases were slightly higher in ferritin H, especially in SH-SY5Y (1.73 ± 0.58 A.U. and $1.74 \pm$

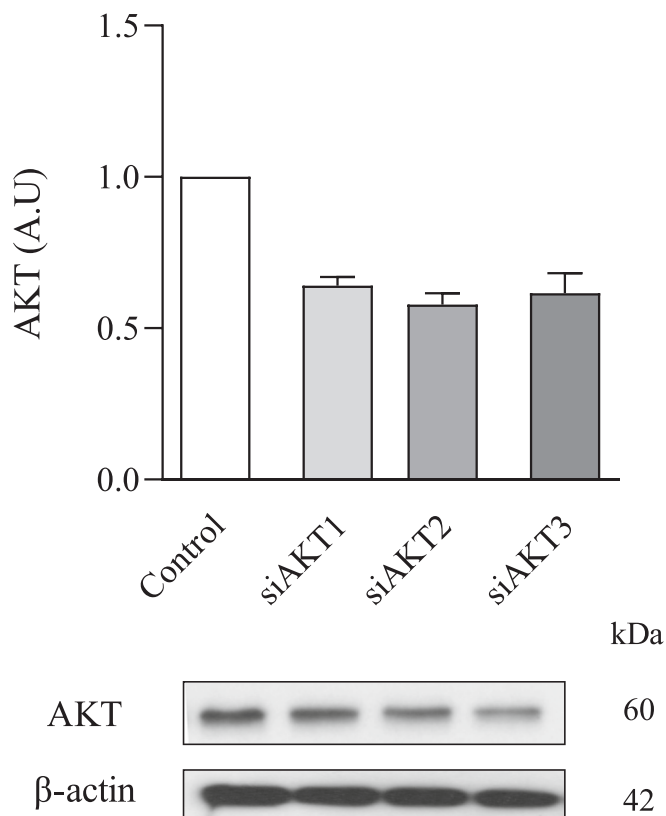


Fig. 6. Effects of siRNA against AKT1, AKT2, and AKT3 on AKT protein level. The assessment of the effect of AKT kinase silencing (siRNA AKT1, AKT2, AKT3) on the proteins of iron metabolism was accompanied by controlling the efficiency of the transfection. Representative immunoblot for stable cell line SH-SY5Y pcDNA3.1 transfected with siRNA against AKT1, AKT2, and AKT3, respectively. AKT1, AKT2, and AKT3 densitometric scanning data after correction for β -actin loading control are on top of AKT immunoreactive bands. Bar graphs of the figure present a change in protein levels as the mean \pm SEM of four independent experiments relative to the control.

0.79 A.U., for siAKT 2 and 3 respectively, Fig. 7 B) than in C_2C_{12} (1.4 \pm 0.36 A.U. and 1.63 \pm 0.46 A.U., for siAKT 2 and 3 respectively, Fig. S3 B).

The transfection of cells with siAKT led to an increase in the level of PCBP1 in all three silencing AKT isoforms. The highest increase was observed in siAKT2 in both SH-SY5Y pcDNA3.1 (Fig. 7 C) and C_2C_{12} pcDNA3.1 (Fig. S4 A) cell lines compared to control (1.42 \pm 0.27 and 2.48 A.U.).

In SH-SY5Y pcDNA3.1, the TfR1 level increased in siRNA AKT1 (1.54 \pm 0.23 A.U.), siRNA AKT2 (1.78 \pm 0.24 A.U.), siRNA AKT3 (1.68 \pm 0.24 A.U.) compared to control (Fig. 7 D).

3.8. Akt inactivation induced changes in iron-exporting proteins in SH-SY5Y and C_2C_{12} cells

Interestingly, down-regulation of AKT (siRNA AKT1, AKT2, AKT3) led to a slight increase of PCBP2 in C_2C_{12} pcDNA3.1 (1.47, 1.09, 1.43 A.U., respectively, Fig. S4 B), but not in SH-SY5Y pcDNA3.1 where we even observed a slight decrease of the protein (0.76 \pm 0.11, 0.71 \pm 0.15, 0.68 \pm 0.16 A.U., respectively, Fig. 8A). What is more, the decrease of PCBP2 was accompanied by a slight decrease of ferroportin in both cell lines. The decrease was slightly higher in SH-SY5Y pcDNA3.1 (0.81 \pm 0.17, 0.70 \pm 0.17, 0.72 \pm 0.23 A.U., for siRNA AKT1, AKT2, AKT3 respectively, Fig. 8 B), than in C_2C_{12} pcDNA3.1 (0.89 \pm 0.08, 0.82 \pm 0.05, 0.79 \pm 0.02 A.U., for siRNA AKT 1, AKT 2, AKT 3 respectively, Fig. S4 C).

In SH-SY5Y pcDNA3.1, the downregulation of AKT2 and AKT3 led to an increase in APP (1.23 \pm 0.47 and 1.33 \pm 0.63 A.U., respectively, Fig. 8 C). Interestingly, in C_2C_{12} pcDNA3.1, only a small increase in APP was observed (1.07 \pm 0.06 A.U.) in cells treated with siRNA AKT1, while in siRNA AKT 2 and AKT 3, a slight drop in was noticed (0.56 \pm 0.48 vs. 0.53 \pm 0.59 A. U., respectively, Fig. S4 D). Moreover, the inactivation of AKT (AKT1, AKT2 AKT3) kinases led to a higher synthesis of the TAU protein, compared to control, in SH-SY5Y pcDNA3.1 cells (1.34 \pm 0.30, 1.3 \pm 0.20, 1.59 \pm 0.38 A.U., respectively, Fig. 8D.)

3.9. Silencing of APP upregulates ferritin proteins in SH-SY5Y and C_2C_{12} cells

Transfection of stable cell lines SH-SY5Y pcDNA3.1 (Fig. 9A) and C_2C_{12} pcDNA3.1 (Fig. S5 A) with siRNA against APP led to down-regulation of APP. In addition, the down-regulation of APP led to an increase in the level of both ferritin subunits. In SH-SY5Y pcDNA3.1, there were almost 5 times higher levels of both proteins (4.2 \pm 1.93 and 5.1 \pm 3.8 A.U., respectively for ferritin L and ferritin H, Fig. 9B and C), while in C_2C_{12} pcDNA3.1, the level of ferritin L and H was not significantly changed compared to the control (1.06 \pm 0.06 vs. 1.05 \pm 0.05 A. U., respectively, Fig. S5 B and Fig. S5 C).

Interestingly, in the SH-SY5Y pcDNA3.1 cell line, there was a slight increase in FPN1 (1.11 \pm 0.34 A.U., Fig. 9 D), while in the C_2C_{12} pcDNA3.1 cell line, there was a slight drop in FPN1 (0.96 \pm 0.12 A.U., Fig. S5 D).

4. Discussion

4.1. Effect of ALS disease on Iron metabolism proteins in ALS mice

We have shown previously that the progression of ALS is associated with increased skeletal muscle iron accumulation. This process is mediated by the inactivation of AKT kinase, which is responsible for the upregulation of ferritin, possibly leading to iron accumulation [13,25]. In this study, we assume that the role of iron in the pathogenesis of ALS will be confirmed if swim training, known to increase the life span of transgenic animals [4], is associated with the amelioration of iron metabolism. We confirmed that the progress of the disease in the animal model is associated with changes in proteins involved in iron metabolism and a decrease in the level of the active form of kinase AKT (p-AKT). We show that along with disease progression, the proteins involved in iron import and storage increase (TfR1, PCBP1 ferritin L and H), and proteins responsible for iron export decrease (TAU, APP, FPN1) in the untrained ONSET and TERMINAL stage of the disease. As we assumed, in skeletal muscle derived from the trained mice, many changes in proteins involved in iron metabolism have been reversed. Thus, the main goal of the present study was to gain insights into whether changes in iron metabolism are a cause or the result of the disease. First of all, we observed an increase in skeletal muscle iron content at the onset of the disease, and it was associated with significantly increased levels of both ferritin subunits. A similar trend was observed in increased quadriceps muscle Fe concentration in mice with the first disease symptoms [26]. It is important to note that iron stored in ferritin is only a part of the iron in the skeletal muscle, whereas most is a portion of metalloproteins such as myoglobin, cytochromes, and others [27].

4.2. Effect of swim training on iron metabolism proteins in ALS mice

The ferritin protein level is strictly related to intracellular iron. A decrease in ferritin H and L after swim training indicates that changes in stored iron are essential. Its increase activates iron-responding proteins, which results in ferritin upregulation. Conversely, a decrease in cell iron leads to the down-regulation of ferritin [28]. Besides, experiments on cell culture demonstrated that ferritin overexpression leads to

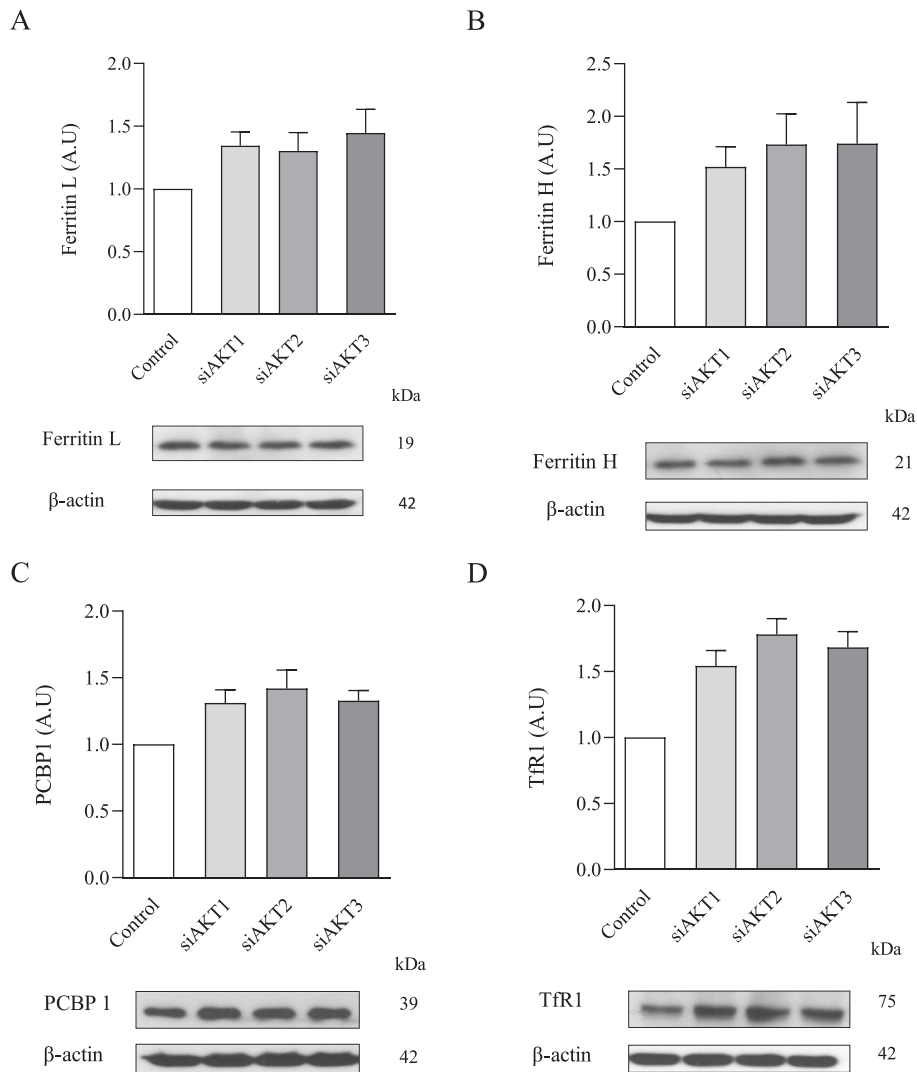


Fig. 7. Effects of AKT silencing on proteins involved in iron import and storage in SH-SY5Y cells.

Ferritin L (A), Ferritin H (B), PCBP1 (C), and TfR1 (D) of stable cell line SH-SY5Y pcDNA3.1 transfected with siRNA against AKT1, AKT2, and AKT3, respectively. Changes in the densitometry levels of particular proteins were normalized against β -actin. Bar graphs of the figure present a change in protein levels as the mean \pm SEM of four independent experiments relative to the control.

intracellular iron accumulation, possibly by decreasing LIP and inducing iron import into cells [29]. On the one hand, ferritin stores iron and protects cells from toxicity; on the other hand, activation of stress protein kinases can lead to ferritin degradation and iron toxicity [30]. Thus, understanding the mechanism of iron accumulation in a tissue is very important. After swim training, several proteins involved in iron metabolism have been measured to determine the mechanism of decreasing skeletal muscle ferritin (iron). TfR1, a protein involved in iron transport into a cell, was slightly upregulated in ONSET of ALS, but unexpectedly, swim training increased its level. Conversely, PCBP1, an iron chaperon delivering iron to ferritin and other proteins [31,32], was strongly upregulated at ONSET of ALS, and the training reverses this change. It is known that human cells lacking PCBP1 load less iron into ferritin [31]; thus, it can be expected that the observed decrease in PCBP1 after swim training can be responsible for a decrease of iron import to the muscles and a decrease in ferritin level. Conversely, another iron chaperon, PCBP2, involved in iron export from a cell, which has been demonstrated to deliver iron to ferroportin, was strongly upregulated after the training. It has been shown that silencing of PCBP2 expression suppressed FPN1 iron export [33]. Thus, its upregulation should increase iron export and lower its tissue level. Moreover, PCBP2 is down-

regulated in degenerating neurons in ALS, which confirms our observations [34].

A similar increase of TAU and APP after the swim training was observed at ONSET of the disease, but there were no changes in FPN1. It has been shown that APP stabilizes the cell surface ferroportin, thus stimulating iron export [35,36].

APP knockout markedly exaggerates age-dependent brain iron accumulation [37]. Besides, the loss of TAU protein has been shown to cause iron retention in neurons by decreasing the surface trafficking of APP [38]. We have shown previously, in the rat model of ALS, that the progress of the disease was associated with an increase in APP protein level, accompanied by an increase in ferritin [13]. Thus, it can be concluded that swim training reduced skeletal muscle ferritin iron content by upregulating proteins involved in iron export from the muscle and down-regulating PCBP1.

4.3. Effect of AKT kinase and APP knockdown on iron metabolism proteins in cells

In order to get insight into observed changes in iron metabolism induced by swim training related to a decreased activity form of kinase

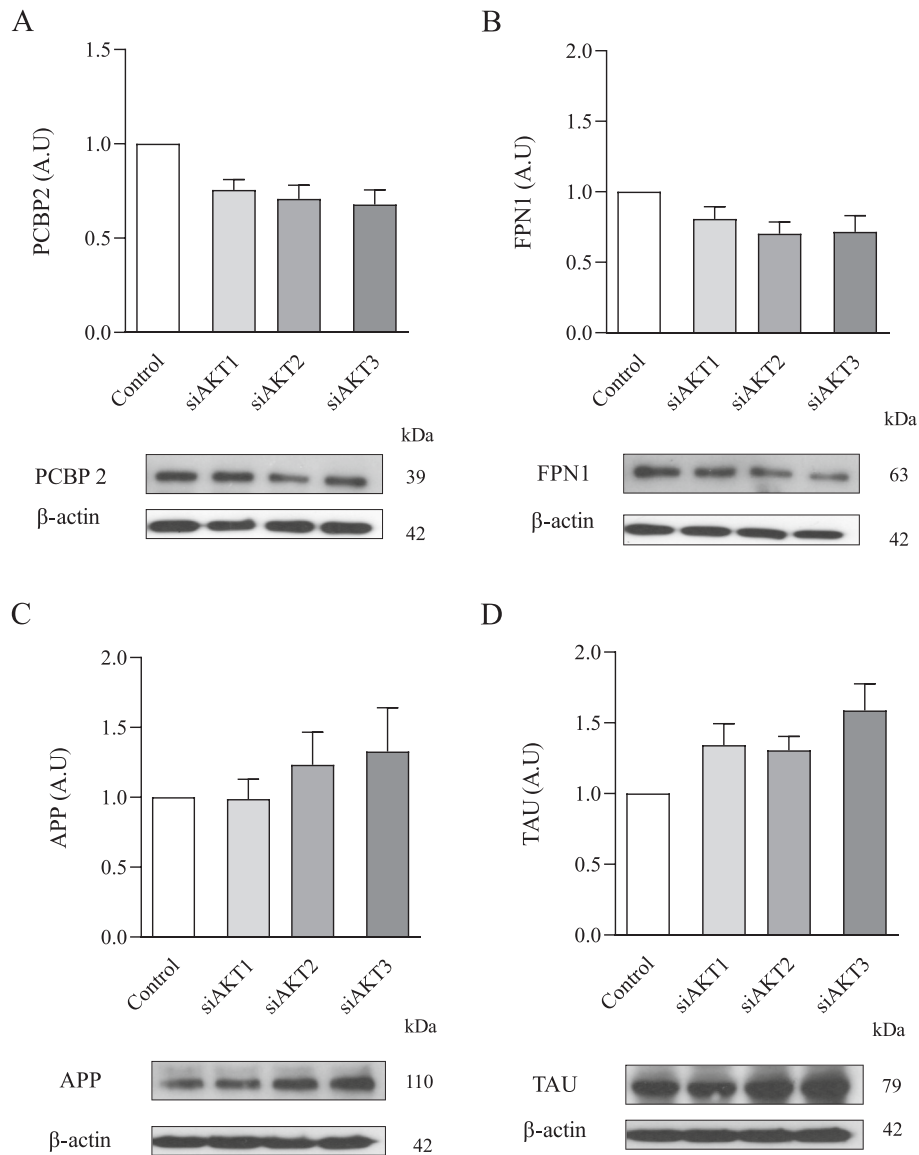


Fig. 8. Effects of AKT silencing on proteins involved in iron export in SH-SY5Y cells.

PCBP2 (A), FPN1 (B), APP (C), and TAU (D) of stable cell line SH-SY5Y pCDNA3.1 transfected with siRNA against AKT1, AKT2, and AKT3, respectively. Changes in the densitometry levels of particular proteins were normalized against β -actin. Bar graphs of the figure present a change in protein levels as the mean \pm SEM of four independent experiments relative to the control.

AKT, experiments on cell culture SH-SY5Y and C₂C₁₂ have been performed. Silencing of AKT1, AKT2, and AKT3, respectively, upregulated ferritin L and H in SH-SY5Y and PCBP1 in both cell lines while suppressing PCBP2 expression in SH-SY5Y. These changes largely mirror those observed in the muscles of transgenic animals, confirming the role of AKT kinase in regulating iron metabolism. Conversely, silencing AKT kinases increased APP, TAU, and TfR1 expression and decreased FPN1 levels. The progress of ALS in the mouse model was associated with a decrease in APP level at the ONSET and increased at the TERMINAL stage of the disease, while in the rat model, the increase has been observed along with disease progression, which confirms our experimental cellular data [13]. Despite some differences between animal models and cell line experiments, the final effects are the same- upregulation of ferritin and increased iron accumulation. It happens because iron cannot be exported during the progression of the disease in skeletal muscle because of a decrease in proteins collaborating with FPN1, like TAU and APP. In the case of cell culture with silenced AKT, iron cannot be transported outside the cell because PCBP2 and FPN1 are down-regulated. The exact mechanism of the AKT signaling pathway to

induce changes in iron metabolism is unknown. Previously, we demonstrated that the transcriptional factor mediates the observed upregulation of ferritin in cells with silenced AKT - forkhead box O3a [13]. Conversely, increased ferritin H has been shown to reduce the labile iron pool (LIP). The expression of proteins like TfR1 and APP is controlled by LIP [39]. Moreover, the expression of proteins like APP and ferritin can be upregulated by inflammatory cytokines [39]. Thus, observed differences between skeletal muscles and cell lines can result from multiplied interactions, which are difficult to predict, especially in vivo conditions. Moreover, to confirm the role of APP, we transiently transfected the SH-SY5Y cell line with APP siRNA and observed an increase in ferritin L and H, indicating an iron accumulation, which confirms previous reports [33].

5. Conclusions

In summary, ALS induces the down-regulation of AKT protein, related to the up-regulation of iron import and storage, but not proteins involved in iron export. Our study also demonstrated that swim training

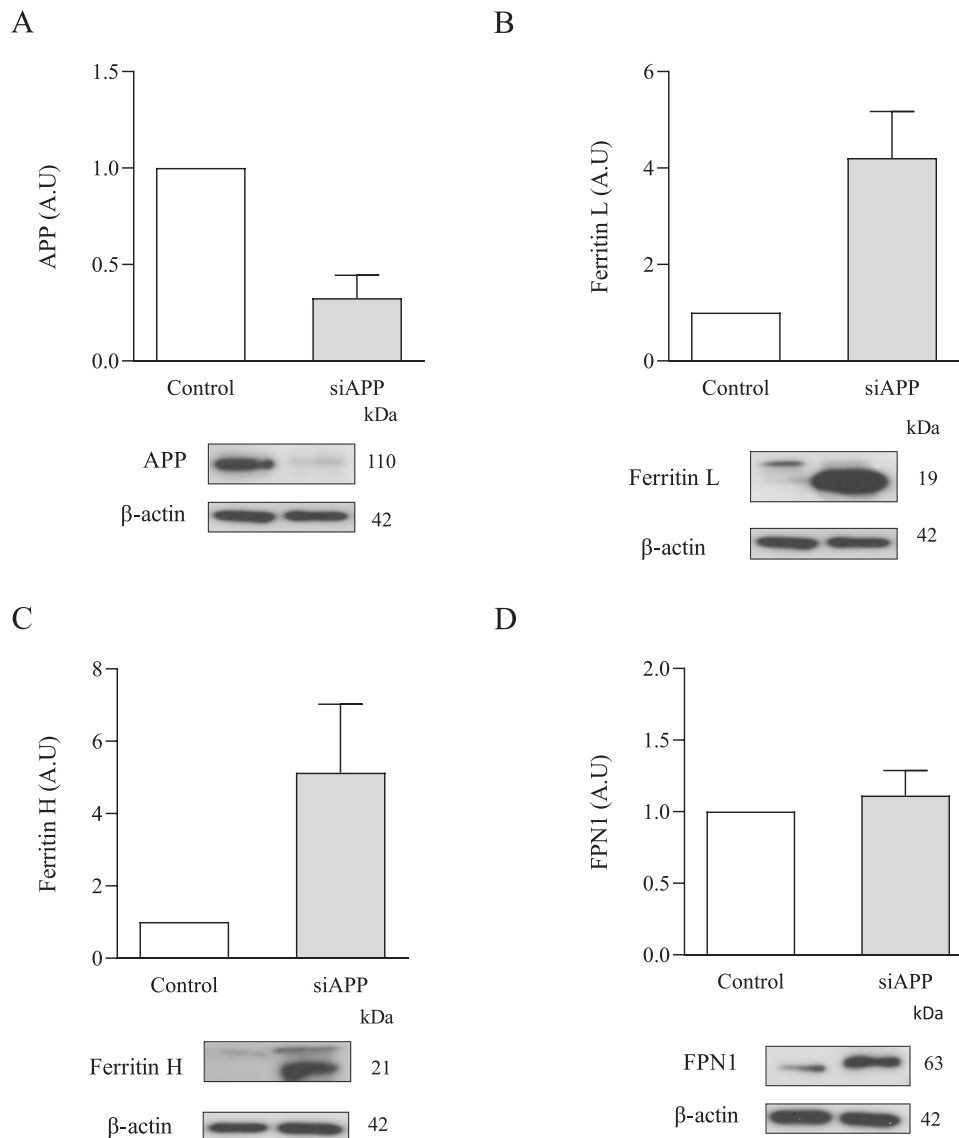


Fig. 9. Effects of APP silencing on proteins involved in iron metabolism SH-SY5Y cells.

APP (A), Ferritin L (B), Ferritin H (C), and FPN1 (D) of stable cell line SH-SY5Y pcDNA3.1 transfected with siRNA against APP. Changes in the densitometry levels of particular proteins were normalized against β -actin. Bar graphs of the figure present a change in protein levels as the mean \pm SEM of four independent experiments relative to the control.

reverses some deleterious changes in skeletal muscle iron metabolism related to the AKT kinase signaling pathway.

To the best of our knowledge, this is the first work demonstrating that AKT modulates these proteins' levels. Thus, we believe that the results of this study may have much broader implications not only related to iron metabolism.

Ethics approval

All experimental procedures were performed in accordance with European animal research laws (European Communities Council Directive 2010/63/EU). The experiments with animals were approved by the Local Ethics Committee (Resolution No. 11/2013) and the Polish Ministry of the Environment (Decision No. 155/2012).

Funding

This study was supported by grants from the National Science Centre, Poland (DEC-2013/09/NZ7/02538, 2018/02/X/NZ3/00444 and 2020/

39/B/NZ7/03366).

CRediT authorship contribution statement

Małgorzata Halon-Golabek: Conceptualization, Data curation, Formal analysis, Funding acquisition, Investigation, Visualization, Writing – original draft. **Damian Jozef Flis:** Conceptualization, Data curation, Formal analysis, Investigation, Validation, Visualization, Writing – original draft. **Hans Zischka:** Investigation, Validation, Writing – review & editing. **Banu Akdogan:** Investigation, Validation, Writing – review & editing. **Mariusz Roman Wieckowski:** Data curation, Methodology, Visualization, Writing – review & editing. **Jedrzej Antosiewicz:** Conceptualization, Formal analysis, Project administration, Supervision, Writing – original draft. **Wiesław Ziolkowski:** Conceptualization, Formal analysis, Funding acquisition, Supervision, Writing – original draft.

Declaration of competing interest

The authors have no relevant financial or non-financial interests to disclose.

Data availability

The data analyzed during the current study are available from the corresponding author upon reasonable request.

Acknowledgements

The graphical abstract and [Scheme 1](#) were created with [BioRender.com](#).

References

- W. Robberecht, T. Philips, The changing scene of amyotrophic lateral sclerosis, *Nat. Rev. Neurosci.* 14 (2013) 248–264, <https://doi.org/10.1038/nrn3430>.
- L.P. Rowland, Diagnosis of amyotrophic lateral sclerosis, *J. Neurol. Sci.* 160 (Suppl. 1) (1998) S6–24, [https://doi.org/10.1016/s0022-510x\(98\)00193-2](https://doi.org/10.1016/s0022-510x(98)00193-2).
- K. Cieminski, D.J. Flis, K. Dzik, J.J. Kaczor, E. Czyrko, M. Halon-Golabek, M. R. Wieckowski, J. Antosiewicz, W. Ziolkowski, Swim training affects Akt signaling and ameliorates loss of skeletal muscle mass in a mouse model of amyotrophic lateral sclerosis, *Sci. Rep.* 11 (2021) 20899, <https://doi.org/10.1038/s41598-021-00319-1>.
- S. Deforges, J. Branchu, O. Biondi, C. Grondard, C. Pariset, S. Lecolle, P. Lopes, P. Vidal, C. Chanoine, F. Charbonnier, Motoneuron survival is promoted by specific exercise in a mouse model of amyotrophic lateral sclerosis, *J. Physiol.* 587 (2009) 3561–3572, <https://doi.org/10.1113/jphysiol.2009.169748>.
- D.J. Flis, K. Dzik, J.J. Kaczor, K. Cieminski, M. Halon-Golabek, J. Antosiewicz, M. R. Wieckowski, W. Ziolkowski, Swim training modulates mouse skeletal muscle energy metabolism and ameliorates reduction in grip strength in a mouse model of amyotrophic lateral sclerosis, *Int. J. Mol. Sci.* 20 (2019), <https://doi.org/10.3390/ijms20020233>.
- D.J. Flis, K. Dzik, J.J. Kaczor, M. Halon-Golabek, J. Antosiewicz, M.R. Wieckowski, W. Ziolkowski, Swim training modulates skeletal muscle energy metabolism, oxidative stress, and mitochondrial cholesterol content in amyotrophic lateral sclerosis mice, *Oxid Med Cell Longev* 2018 (2018) 5940748, <https://doi.org/10.1155/2018/5940748>.
- S.Y. Jeong, K.I. Rathore, K. Schulz, P. Ponka, P. Arosio, S. David, Dysregulation of iron homeostasis in the CNS contributes to disease progression in a mouse model of amyotrophic lateral sclerosis, *J. Neurosci.* 29 (2009) 610–619.
- C. Moreau, V. Danel, J.C. Devedjian, G. Grolez, K. Timmerman, C. Laloux, M. Petraut, F. Gouel, A. Jonneaux, M. Duthheil, C. Lachaud, R. Lopes, G. Kuchcinski, F. Auger, M. Kyheng, A. Duhamel, T. Perez, P.F. Pradat, H. Blasco, C. Veyrat-Durebex, P. Corcia, P. Oeckl, M. Otto, L. Dupuis, G. Garcon, L. Defebvre, Z.I. Cabantchik, J. Duce, R. Bordet, D. Devos, Could conservative iron chelation lead to neuroprotection in amyotrophic lateral sclerosis? *Antioxid. Redox Signal.* 29 (2018) 742–748, <https://doi.org/10.1089/ars.2017.7493>.
- B. Zhang, P.P. Wang, K.L. Hu, L.N. Li, X. Yu, Y. Lu, H.S. Chang, Antidepressant-like effect and mechanism of action of Honokiol on the mouse lipopolysaccharide (LPS) depression model, *Molecules* 24 (2019), <https://doi.org/10.3390/molecules24112035>.
- A.K. Malik, K.E. Flock, C.L. Godavarthi, H.H. Loh, J.L. Ko, Molecular basis underlying the poly C binding protein 1 as a regulator of the proximal promoter of mouse mu-opioid receptor gene, *Brain Res.* 1112 (2006) 33–45, <https://doi.org/10.1016/j.brainres.2006.07.019>.
- J. Huang, J. Simcox, T.C. Mitchell, D. Jones, J. Cox, B. Luo, R.C. Cooksey, L. G. Boros, D.A. McClain, Iron regulates glucose homeostasis in liver and muscle via AMP-activated protein kinase in mice, *FASEB J.* 27 (2013) 2845–2854, <https://doi.org/10.1096/fj.12-216929>.
- P. Ponka, Hereditary causes of disturbed iron homeostasis in the central nervous system, *Ann. N. Y. Acad. Sci.* 1012 (2004) 267–281, <https://doi.org/10.1196/annals.1306.022>.
- M. Halon-Golabek, A. Borkowska, J.J. Kaczor, W. Ziolkowski, D.J. Flis, N. Knap, K. Kasperuk, J. Antosiewicz, hmSOD1 gene mutation-induced disturbance in iron metabolism is mediated by impairment of Akt signalling pathway, *J. Cachexia. Sarcopenia Muscle* 9 (2018) 557–569, <https://doi.org/10.1002/jcsm.12283>.
- A. Borkowska, W. Ziolkowski, K. Kaczor, A. Herman-Antosiewicz, N. Knap, A. Wronska, J. Antosiewicz, Homocysteine-induced decrease in HUVEC cells' resistance to oxidative stress is mediated by Akt-dependent changes in iron metabolism, *Eur. J. Nutr.* 60 (2021) 1619–1631, <https://doi.org/10.1007/s00394-020-02360-8>.
- L. Zhao, N. Yang, Y. Song, H. Si, Q. Qin, Z. Guo, Effect of iron overload on endothelial cell calcification and its mechanism, *Ann Transl Med* 9 (2021) 1658, <https://doi.org/10.21037/atm-21-5666>.
- X. Sun, T. Xia, S. Zhang, J. Zhang, L. Xu, T. Han, H. Xin, Hops extract and xanthohumol ameliorate bone loss induced by iron overload via activating Akt/GSK3beta/Nrf2 pathway, *J. Bone Miner. Metab.* 40 (2022) 375–388, <https://doi.org/10.1007/s00774-021-01295-2>.
- K.M. Nicholson, N.G. Anderson, The protein kinase B/Akt signalling pathway in human malignancy, *Cell. Signal.* 14 (2002) 381–395, [https://doi.org/10.1016/s0898-6568\(01\)00271-6](https://doi.org/10.1016/s0898-6568(01)00271-6).
- C. Deseille, S. Deforges, O. Biondi, L. Houdebine, D. D'Amico, A. Lamaziere, C. Caradeuc, G. Bertho, G. Bruneteau, L. Weill, J. Bastin, F. Djouadi, F. Salachas, P. Lopes, C. Chanoine, C. Massaad, F. Charbonnier, Specific physical exercise improves energetic metabolism in the skeletal muscle of amyotrophic-lateral-sclerosis mice, *Front. Mol. Neurosci.* 10 (2017) 332, <https://doi.org/10.3389/fnmol.2017.00332>.
- J. Kortas, A. Kuchta, K. Prusik, K. Prusik, E. Ziemann, S. Labudda, A. Cwiklinska, E. Wiecezorek, M. Jankowski, J. Antosiewicz, Nordic walking training attenuation of oxidative stress in association with a drop in body iron stores in elderly women, *Biogerontology* 18 (2017) 517–524, <https://doi.org/10.1007/s10522-017-9681-0>.
- J. Kortas, K. Prusik, D. Flis, K. Prusik, E. Ziemann, N. Leaver, J. Antosiewicz, Effect of Nordic walking training on iron metabolism in elderly women, *Clin. Interv. Aging* 10 (2015) 1889–1896, <https://doi.org/10.2147/CIA.S90413>.
- K. Cieminski, D.J. Flis, K.P. Dzik, J.J. Kaczor, M.R. Wieckowski, J. Antosiewicz, W. Ziolkowski, Swim training affects on muscle lactate metabolism, nicotinamide adenine dinucleotides concentration, and the activity of NADH shuttle enzymes in a mouse model of amyotrophic lateral sclerosis, *Int. J. Mol. Sci.* 23 (2022), <https://doi.org/10.3390/ijms231911504>. ARTN 11504.
- M.J. Hamadeh, M.C. Rodriguez, J.J. Kaczor, M.A. Tarnopolsky, Caloric restriction transiently improves motor performance but hastens clinical onset of disease in the cu/Zn-superoxide dismutase mutant G93A mouse, *Muscle Nerve* 31 (2005) 214–220, <https://doi.org/10.1002/mus.20255>.
- H. Zischka, J. Lichtmanegger, S. Schmitt, N. Jagemann, S. Schulz, D. Wartini, L. Jennen, C. Rust, N. Laroche, L. Galluzzi, V. Chajes, N. Bandow, V.S. Gilles, A. A. DiSpirito, I. Esposito, M. Goettlicher, K.H. Sumner, G. Kroemer, Liver mitochondrial membrane crosslinking and destruction in a rat model of Wilson disease, *J. Clin. Invest.* 121 (2011) 1508–1518, <https://doi.org/10.1172/JCI45401>.
- M.P. Weekes, P. Tomasec, E.L. Huttlin, C.A. Fielding, D. Nusinow, R.J. Stanton, E. C.Y. Wang, R. Aicheler, I. Murrell, G.W.G. Wilkinson, P.J. Lehner, S.P. Gygi, Quantitative temporal viromics: an approach to investigate host-pathogen interaction, *Cell* 157 (2014) 1460–1472, <https://doi.org/10.1016/j.cell.2014.04.028>.
- M. Halon, A. Sielicka-Dudzina, M. Wozniak, W. Ziolkowski, W. Nyka, M. Herbig, P. Grieb, A. Figarski, J. Antosiewicz, Up-regulation of ferritin ubiquitination in skeletal muscle of transgenic rats bearing the G93A hmSOD1 gene mutation, *Neuromuscul. Disord.* 20 (2010) 29–33.
- T.G. Enge, H. Erroyd, D.F. Jolley, J.J. Yerbury, B. Kalmar, A. Dosseto, Assessment of metal concentrations in the SOD1(G93A) mouse model of amyotrophic lateral sclerosis and its potential role in muscular denervation, with particular focus on muscle tissue, *Mol. Cell. Neurosci.* 88 (2018) 319–329, <https://doi.org/10.1016/j.mcn.2018.03.001>.
- P. Buratti, E. Gammella, I. Rybinska, G. Cairo, S. Recalcati, Recent advances in Iron metabolism: relevance for health, exercise, and performance, *Med. Sci. Sports Exerc.* 47 (2015) 1596–1604, <https://doi.org/10.1249/MSS.0000000000000593>.
- D.B. Kell, Iron behaving badly: inappropriate iron chelation as a major contributor to the aetiology of vascular and other progressive inflammatory and degenerative diseases, *BMC Med. Genomics* 2 (2009) 2, <https://doi.org/10.1186/1755-8794-2-2>.
- A. Cozzi, B. Corsi, S. Levi, P. Santambrogio, A. Albertini, P. Arosio, Overexpression of wild type and mutated human ferritin H-chain in HeLa cells: in vivo role of ferritin ferroxidase activity, *J. Biol. Chem.* 275 (2000) 25122–25129, <https://doi.org/10.1074/jbc.M003797200>.
- A. Borkowska, U. Popowska, J. Spodnik, A. Herman-Antosiewicz, M. Wozniak, J. Antosiewicz, JNK/p66Shc/ITCH signaling pathway mediates angiotensin II-induced ferritin degradation and labile Iron Pool increase, *Nutrients* 12 (2020), <https://doi.org/10.3390/nu12030668>.
- H. Shi, K.Z. Bencze, T.L. Stemmler, C.C. Philpott, A cytosolic iron chaperone that delivers iron to ferritin, *Science* 320 (2008) 1207–1210, <https://doi.org/10.1126/science.1157643>.
- A.G. Frey, A. Nandal, J.H. Park, P.M. Smith, T. Yabe, M.S. Ryu, M.C. Ghosh, J. Lee, T.A. Rouault, M.H. Park, C.C. Philpott, Iron chaperones PCBP1 and PCBP2 mediate the metallation of the dinuclear iron enzyme deoxyhypusine hydroxylase, *Proc. Natl. Acad. Sci. U. S. A.* 111 (2014) 8031–8036, <https://doi.org/10.1073/pnas.1402732111>.
- I. Yanatori, D.R. Richardson, K. Imada, F. Kishi, Iron export through the transporter Ferroportin 1 is modulated by the Iron chaperone PCBP2, *J. Biol. Chem.* 291 (2016) 17303–17318, <https://doi.org/10.1074/jbc.M116.721936>.
- M. Yoshimura, H. Honda, N. Sasagasako, S. Mori, H. Hamasaki, S.O. Suzuki, T. Ishii, T. Ninomiya, J.I. Kira, T. Iwaki, PCBP2 is downregulated in degenerating neurons and rarely observed in TDP-43-positive inclusions in sporadic amyotrophic lateral sclerosis, *J. Neuropathol. Exp. Neurol.* 80 (2021) 220–228, <https://doi.org/10.1093/jnen/nlaa148>.
- R.C. McCarthy, D.J. Kosman, Mechanisms and regulation of iron trafficking across the capillary endothelial cells of the blood-brain barrier, *Front. Mol. Neurosci.* 8 (2015) 31, <https://doi.org/10.3389/fnmol.2015.00031>.
- B.X. Wong, A. Tsatsanis, L.Q. Lim, P.A. Adlard, A.I. Bush, J.A. Duce, beta-amyloid precursor protein does not possess ferroxidase activity but does stabilize the cell surface ferrous iron exporter ferroportin, *PLoS One* 9 (2014) e114174, <https://doi.org/10.1371/journal.pone.0114174>.
- A.A. Belaidi, A.P. Gunn, B.X. Wong, S. Ayton, A.T. Appukuttan, B.R. Roberts, J. A. Duce, A.I. Bush, Marked age-related changes in brain Iron homeostasis in

- amyloid protein precursor knockout mice, *Neurotherapeutics* 15 (2018) 1055–1062, <https://doi.org/10.1007/s13311-018-0656-x>.
- [38] P. Lei, S. Ayton, D.I. Finkelstein, L. Spoerri, G.D. Ciccotosto, D.K. Wright, B. X. Wong, P.A. Adlard, R.A. Cherny, L.Q. Lam, B.R. Roberts, I. Volitakis, G.F. Egan, C.A. McLean, R. Cappai, J.A. Duce, A.I. Bush, Tau deficiency induces parkinsonism with dementia by impairing APP-mediated iron export, *Nat. Med.* 18 (2012) 291–295, <https://doi.org/10.1038/nm.2613>.
- [39] J.T. Rogers, A.I. Bush, H.H. Cho, D.H. Smith, A.M. Thomson, A.L. Friedlich, D. K. Lahiri, P.J. Leedman, X. Huang, C.M. Cahill, Iron and the translation of the amyloid precursor protein (APP) and ferritin mRNAs: riboregulation against neural oxidative damage in Alzheimer's disease, *Biochem. Soc. Trans.* 36 (2008) 1282–1287, <https://doi.org/10.1042/BST0361282>.